Volume 3
Number 24
21 December 2022
Pages 8805–9120

Materials Advances

rsc.li/materials-advances

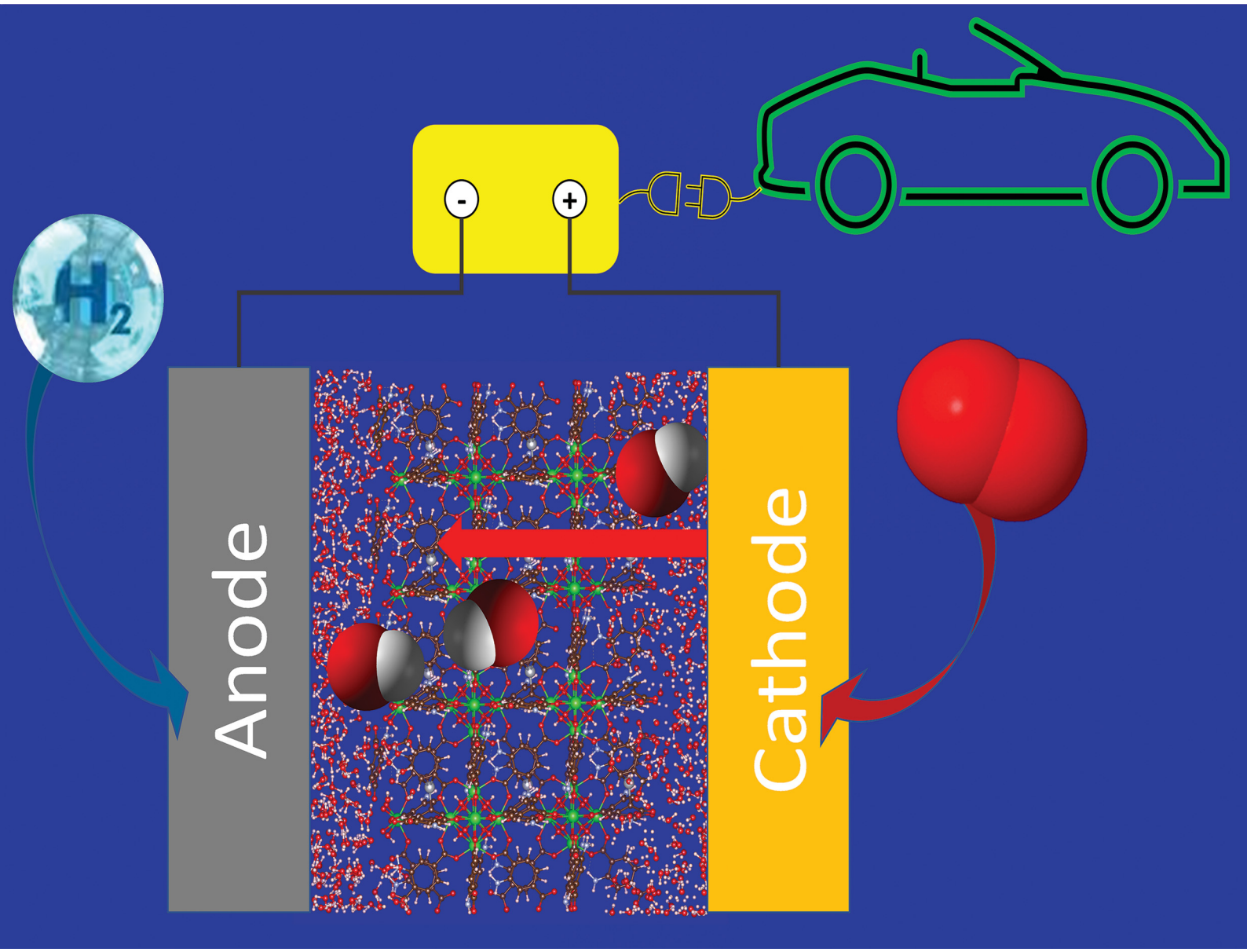

ISSN 2633-5409

ROYAL SOCIETY OF CHEMISTRY

REVIEW ARTICLE
Maria-Magdalena Titirici and Petra Ágota Szilágyi
Hydroxide ion-conducting metal–organic frameworks for anion-exchange membrane applications

Materials Advances

ROYAL SOCIETY OF CHEMISTRY

REVIEW

View Article Online
View Journal | View Issue

Cite this: *Mater. Adv.*, 2022, 3, 8815

Hydroxide ion-conducting metal–organic frameworks for anion-exchange membrane applications

Maria-Magdalena Titirici [a] and Petra Ágota Szilágyi *[b]

Received 31st August 2022,
Accepted 28th September 2022

DOI: 10.1039/d2ma00880g

rsc.li/materials-advances

With the increasing demand for green energy, there is a great urgency to develop perm-selective, economical and robust membranes for applications in fuel cells. Metal–organic frameworks are attractive materials for this application as they are typically electrically insulating, have tuneable pore size and chemistry – enabling the realisation of specific interactions with the ions -, and their processing technology has recently undergone a tremendous development, allowing for their synthesis as free-standing membranes. This critical review aims at evaluating recent advances in the field of hydroxide-ion conducting metal–organic frameworks for ion-exchange membrane applications. In addition, it will conceptualise the most promising approaches for design, synthesis and processing of the framework-based membranes.

Introduction

There is a scientific and increasingly societal consensus that the current energy paradigm largely based on fossil-fuel combustion for energy provision is unsustainable and it urgently needs to be replaced by renewables. The reason for this is manifold, including the increasingly real problem of climate change, loss of biodiversity, and health concerns, but also the constantly decreasing resources, volatile and unreliable geopolitical issues, as well as fluctuating prices. Renewable energy sources on the other hand are plentiful, and most geographical areas possess significant resources of at least some types of them and the technologies offered by them are increasingly affordable.[1] Renewables are however typically fluxes and as such, they only allow for energy conversion to electricity rather than for storage. On account of their spatial and temporal distribution as well as general intermittence they are not able to provide an even load to demand and thus need to be balanced and, in peak periods, energy storage solutions need to be found.[2] To this end, current technologies typically make use of electrochemical energy storage in the form of batteries. However, it is increasingly apparent that battery technologies alone are not able to afford the energy storage needed for the full transition of the energy landscape; in particular, some applications have characteristic requirements that batteries currently cannot meet, these include heavy-duty vehicles, aviation, naval transport, grid-scale storage, *etc.*[3] For this reason, it is imperative that in conjunction with electrification alternative energy-storage technologies are also developed and marketed. In particular, the production of high energy-density fuels in peak renewable-flux periods is a realistic and desirable energy-storage solution for diverse applications, complementary to battery technologies.

Hydrogen economy

Among high energy-density fuels, hydrogen is highly promising and it has been the subject of significant research interest. Its advantages include the highest energy density of all known substances by weight (120 kJ mol^{-1}) and availability – it is the most common element in the universe, which is within the five most abundant elements on Earth and water in particular is a plentiful source of it. Furthermore, hydrogen is unrivalled in the versatility of ways it may be utilised for energy conversion and storage, combusted,[4] electrochemically oxidised in a fuel cell,[5] and used as a reactant to form fuels such as liquid hydrocarbons,[6] which processes may take place through a variety of reaction types ranging from thermally to (photo-)electrochemically driven reactions. As a matter of fact, the hydrogen economy has been highlighted as particularly appealing as it may be included in a completely carbon-free cycle,[7] provided it is generated photo/electro-chemically, *i.e.* green hydrogen is used. However, safe and green production is not the only challenge needing to be overcome for the hydrogen economy to be a reality, additional challenges include its

[a] *Department of Chemical Engineering, Imperial College London, South Kensington Campus, London, SW7 2AZ, UK*
[b] *Center for Materials Science and Nanotechnology (SMN), Department of Chemistry, University of Oslo, P.O. Box 1033, Blindern, N-0315 Oslo, Norway. E-mail: P.A.Szilagyi@kjemi.uio.no*

low-cost, safe, efficient and effective storage, distribution, and oxidation to water.[8]

Fuel cells

The electrochemical oxidation of hydrogen produces water as the sole product in the electrochemical device of fuel cells. This process is crucial as the combustion of hydrogen is highly exothermic, in fact, it forms an explosive mixture with air in a broad concentration range, which makes its controlled oxidation not only more efficient but also much safer and thus highly desirable.[5] In fuel cells, hydrogen is stripped of electrons on the anode, while oxygen is reduced on the cathode. The two redox reactions (half reactions) are physically separated and the process is accompanied by the flow of electrons from the anode to the cathode on an external circuit. It generates electricity while ions flow between the two electrode sides of the device, which are separated by a semipermeable membrane for charge balancing. Mature fuel cell technology makes use of protons to balance charges by flowing from the anode to the cathode side across a proton conducting membrane, in the proton-exchange membrane fuel cell (PEMFC). In PEMFCs, the processes are as follows:

Anode:	$H_2 \rightarrow 2\ H^+ + 2\ e^-$
Cathode:	$1/2\ O_2 + 2\ e^- + H_2O \rightarrow 2\ OH^-$
Electrolyte:	$H^+ + OH^- \rightarrow H_2O$
Overall:	$H_2 + 1/2\ O_2 \rightarrow H_2O$

Commercial PEMFCs typically feature a Nafion® proton exchange membrane, which boasts high proton conductivity, adequate chemical stability, mechanical robustness, and acceptable costs. However, the integration of polymers into devices causes increasing environmental concerns over the sustainability of polymer manufacturing as well as over their fate beyond disposal.[9,10] It is important to re-iterate that hydrogen and oxygen combine to form an explosive gas mixture in a broad concentration range; therefore, the mixing of the two gases must be avoided at all times. Technically, the gases are introduced into the device *via* separate cell compartments, but it is also important that the dissolved gas molecules do not transfer between the two different compartments through the electrolyte (and the membrane) either. This phenomenon is called crossover, which presents a practical challenge in the development of membranes – ideally they would be perm-selective for protons. However, repulsive interactions with hydrogen molecules are difficult to achieve and in order to avoid H_2 transfer into the cathode side, thicker membranes are typically applied, as a result of which a kinetic barrier to the transfer of unwanted species emerges.[11] This, however, exacerbates issues regarding cost, environmental impact, *etc.* Consequently, viable alternatives are being sought.

Although PEMFCs equipped with Nafion® membranes are a mature commercial technology with fair efficiency, they have the drawback of, because of the ion transport process, requiring a highly acidic, corrosive environment as an electrolyte.[12] Besides the obvious health and safety and environmental issues related to the use of low pH solutions in potential every-day technologies, the strongly acidic environment also requires the use of components that can withstand the corrosive environment, which is a particularly penalising limitation for the electrocatalyst, particularly for the anode, for which the costly and increasingly scarce Pt is employed.[13] However, more earth-abundant, low-cost electrocatalysts, such as Fe or Ni, have been shown to display comparable performance to Pt, when used in an alkaline environment wherein they are sufficiently stable.[14]

Alkaline fuel cells

Alkaline electrolyte conditions are provided in alkaline anion-exchange membrane fuel cells (AAEMFCs), wherein the charge compensating ion transport is accomplished by the migration of hydroxide ions from the cathode side to the anode side. The electrode reactions in AAEMFCs are the same as in PEMFCs in the sense that hydrogen is oxidised on the anode while oxygen is reduced on the cathode to form water molecules (and generate electricity). The conceptual difference lies in the charge balancing ion nature and the direction of the ion transport. As seen before, in the case of PEMFCs, positively charged protons migrate from the anode side to the cathode side, in contrast, for AAEMFCs, negatively charged hydroxide ions are traversing the membrane from the cathode to the anode compartment (Fig. 1).[15] This arrangement presents several advantages, including the possibility to employ cheaper electrocatalysts, the improved oxygen-reduction reaction kinetics in an alkaline medium, and the simpler balance of plant near ambient pressure, and, as the ion transport direction opposes that of the current, lower crossover and electrical drag are expected. Nonetheless, AAEMFC technology is not without its drawbacks, a major disadvantage for the widespread roll-out of the technology being the availability of hydroxide-ion exchange membranes with low cost, high ion conductivity, chemical and mechanical stability, easy processability, *etc.*[16]

It should be emphasised that both PEMFC and AAEFMC technologies are desirable as they enable the use of hydrogen as a fuel, contributing to a radical change in the energy landscape. Although there is a clear prospect of developing more efficient and cost-effective electrocatalysts, both technologies are limited by membranes, and to be specific by the membrane materials themselves, and thus further research efforts are needed in this direction.[17,18] It is for this reason that the exploration and evaluation of other material classes is of great importance and timeliness.

Ion-exchange membranes

In order for a membrane to be viable, they should have the following characteristics: (i) high ion conductivity, protons or hydroxide ions, depending on the medium, (ii) strong chemical and mechanical robustness in the relevant medium, (iii) no

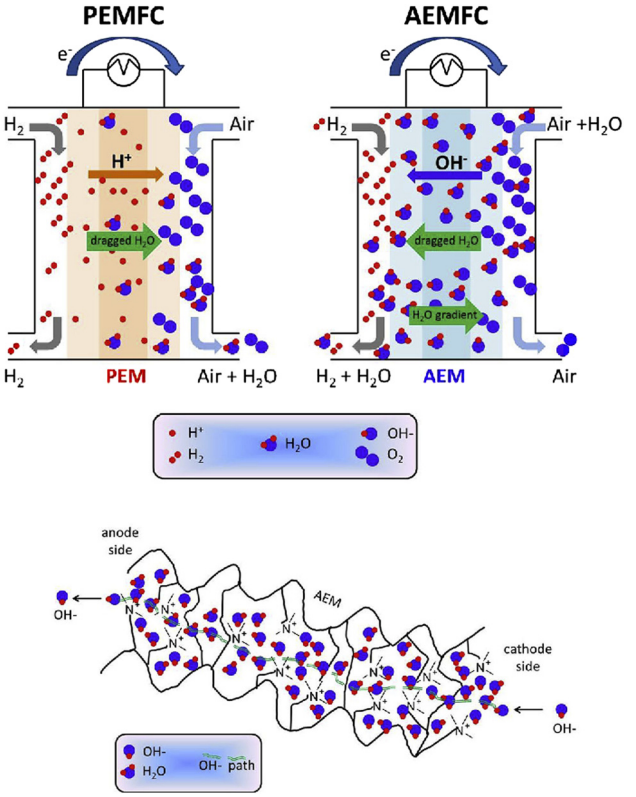

Fig. 1 Schematic of an AEMFC as compared to a PEMFC (top scheme), and of an AEM based on a quaternary ammonium pendant functional group (bottom scheme). Reproduced with permission from ref. 15.

crossover (or minimal), *i.e.* only the transfer of the desired ion occurs through the membrane and not that of any other ions or the reactant hydrogen or oxygen molecules. In particular, as previously explained, the avoidance of reactant crossover is highly important from a safety perspective, (iv) affordability and (v) low environmental footprint. When it comes to properties of the materials, these characteristics translate into (i) vacuous structure, such as porous or channelled, enabling fast ion transport, electronic insulation to avoid short-circuits, (ii) chemical inertness and morphological stability, (iii) selectivity *via* highly specific interactions and/or pore diameters, (iv) scalable synthesis, an abundance of precursors and ease of processing, and (v) ability to be produced under mild conditions using green chemical principles, reactants may be sourced sustainably, easily recyclable, *etc.* In essence, materials classes that may afford the above should be a high priority of research focus for the development of advanced membranes for fuel-cell technologies.

While various material classes are being explored as ion-exchange membranes for fuel-cell applications,[12,19] it is out of the scope of this review paper to evaluate the current state-of-art technology and recent progress in all classes. However, it should be noted that there are two classic material classes that are typically the focus of exploration, *i.e.* organic polymers and ceramics. Polymer-exchange membranes are flexible and easily processed. However, they suffer from stability issues and structural changes occurring in contact with the electrolyte, *e.g.* swelling, and they are typically synthesised in environmentally unsustainable approaches while they also represent significant recycling issues beyond their lifetime.[20] On the other hand, with operating conditions at high temperatures, inorganic ceramic ion-exchange membranes are also investigated, which are chemically robust materials that may be produced from abundant and relatively harmless resources. However, they lack poor processability and some detrimental mechanical characteristics, such as brittleness.[21]

In recent years, hybrid inorganic–organic materials have emerged as potential contenders in the ion-exchange membrane field.[22] Such materials are expected to intrinsically combine the desirable properties of both organic and inorganic materials, such as good mechanical flexibility and robustness, absence of swelling, chemical and structural tuneability, stability and ease of processing. This review explores advances in the design of certain hybrid materials for ion exchange purposes.

Discussion

Metal–organic frameworks

A particular class of intrinsically hybrid materials, which have been attracting tremendous research interest in applications ranging from catalysis, electrochemical energy storage, gas storage and separation, sensing, water harvesting to the removal of toxic waste is metal–organic frameworks (MOFs).[23–31] These materials are composed of inorganic nodes, such as metal cations or oxidic clusters, interconnected by organic linkers, typically polycarboxylates or heterocycles, *via* coordination bonds. When the building blocks self-assemble, they typically form an extended crystalline porous framework (Fig. 2). Taking advantage of both organic and inorganic chemistry, the framework topologies achievable are virtually limitless, and in fact, over 100 000 structures have been reported in the Cambridge Crystallographic Data Centre already.[32]

Importantly, MOFs have an open pore structure interlinked *via* channels, which are all part of the crystal structure; consequently, their geometry and chemistry may be controlled with atomic precision.[33–41] This is a crucial advantage as it provides a way for engineering the interactions of loosely bonded ions with the MOF structure on the surface of the channels across

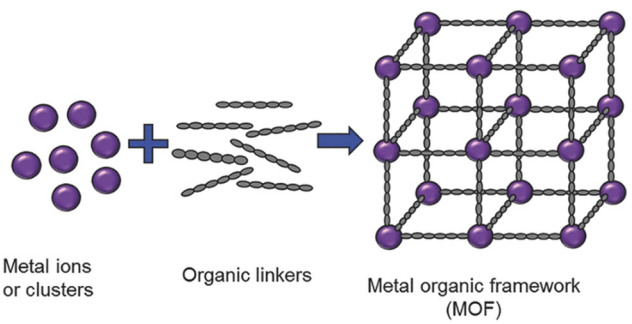

Fig. 2 Generalized scheme for metal–organic framework preparation. Reproduced with permission from ref. 31.

the particles, which in principle should provide an unrivalled approach to control the ion transport. It is for the above reasons that metal–organic frameworks have been the subject of increasing investigations and in effect an emerging class of materials for ion-exchange membranes.[42] Their ability to maximise inherent ion conductivity may be rationalised based on their structural and compositional properties: i) as a consequence of MOFs being formed on a self-assembly of inorganic and organic building blocks, in which the channels are intrinsic features of the crystal structure; they are therefore highly regular and tuneable both topologically and chemically and thus also offer a strict design-driven control over intrinsic ion mobility; ii) the intrinsically porous nature of MOFs offering open channels allows for ion conduction pathways inside the crystallite, restricting the ion transport to the[43] interior to the MOF particles. Therefore, the ion transport inside macroscopic amounts of MOFs may be controlled by the careful design and crystal engineering of MOF lattices in principle. This, in combination with the unrivalled structural and compositional versatility, makes MOFs a highly desirable material class for applications relying on ion conductivity, particularly as ion-exchange membranes in fuel cells.

MOFs for ion-exchange membrane applications

In particular, for MOFs as proton-exchange membranes, there has been a tremendous advance both in terms of fundamental understanding of the underlying processes, experimental characterisation, processing, and development of materials, resulting in recorded proton conductivities exceeding 10^{-2} S cm^{-1} in operational conditions, with viable stabilities and manufacturing approaches, while a deep understanding in the conductivity mechanisms is also being developed, putting MOFs in the vanguard of cutting-edge proton conductor materials. It should be noted that recently there have been a number of excellent authoritative reviews in this field and the readers are encouraged to consult them.[35,36,39,44–51] However, hydroxide-ion conductive MOFs and their membranes are a much less explored area, likely the consequence of the maturity of the PEM-FC technology over that of the AAEM-FC; therefore, it is the latter, which is the focus of the present work.

Challenges

As seen, MOFs are a highly promising material class for ion-exchange membrane applications; nevertheless, some of the intrinsic challenges arising from their chemical composition and physical characteristics need to be considered and applied in the evaluation of their performance. In particular, the stability of MOFs in highly alkaline media is a limiting factor; most metal–organic frameworks feature hard acids in their nodes and therefore combine easily with hydroxide ions, resulting in framework decomposition.[52] Even MOFs considered as highly stable chemically, such as UiO-66(Zr), ZIF-8 or MIL-53(Al), show signs of degradation in alkaline media.[53,54] In order to construct a reliable fuel-cell device, it is indispensable that the MOF-based membrane withstand the harsh conditions, potentially amounting to 6 M KOH,[55] in its pure form, or an alternative processing technique must be developedto improve the frameworks' chemical resistance. Although ion-exchange membranes when integrated into a fuel cell are immersed in a liquid electrolyte, in order to achieve the very high ion conductivity approaching that afforded by the current proton-exchange membrane technology, high intrinsic hydroxide-ion conductivities must be achieved in the frameworks, as it will be seen, current materials offer significantly lower ion conductivities for hydroxide ions than for protons. MOFs are typically synthesised as powders, which form is not useful for membrane production. Recent advances in developing processing and fabrication technologies, such as monolith, thin film, or fibre-mat production give confidence that such challenges regarding the processing of MOFs are easily amenable to membrane formation with controlled porosity and thickness will be overcome.[56–64] It should be noted that with the advent of industrial production of certain MOFs, it has been shown that their production costs can be reduced significantly, as highlighted by recent reports.[65,66] However, to date there is only a handful of commercially available MOFs and their price is currently not competitive with well-established productions such as ceramics or common polymers.

Sustainability issues associated with polymer materials are well known, but it is a less explored area for more recent classes of materials, such as metal–organic frameworks. As a general rule, MOFs are formed of coordinative bonds, which are easier to break than covalent ones and thus the recyclability of MOFs is not such a grave problem. In addition, recent advances in applying green chemical principles for MOF syntheses have paved the way for the emergence of sustainable MOFs, making them a more environmentally benign option so long as their component metals are captured and re-used after their lifespan.[67–70]

Ion transport

In addition to practical considerations, the mechanism through which hydroxide ions are transported within the ion-exchange membrane, and in particular inside the MOF channels needs to be evaluated and quantified. In a general sense, mass transport is described through the self-diffusion coefficient; in porous materials, there are three main mechanisms to mass transport the relative contribution of which depend on the conditions and the host-guest interaction strength: (i) the diffusion of molecules/ions, say when immersed in a solvent or exposed to gas pressure the molecules/ions physically located inside the pores may collide and an effective motion thus takes place down on a concentration gradient; (ii) the Knudsen diffusion, which occurs on the collision of guest molecules/ions with the pore and channel surfaces; and (iii) the surface diffusion, which consists of the adsorption and subsequent desorption of guest particles on a surface site, resulting in effective surface-hopping motions.[71,72]

More to the point of applications in ion-exchange membranes, the transport of ions in the medium of electrolytes needs to be regarded. In the case of proton transport in aqueous solutions, the mobility of protons is exceptionally high, *ca.* and order of magnitude higher than that of Li^+ or

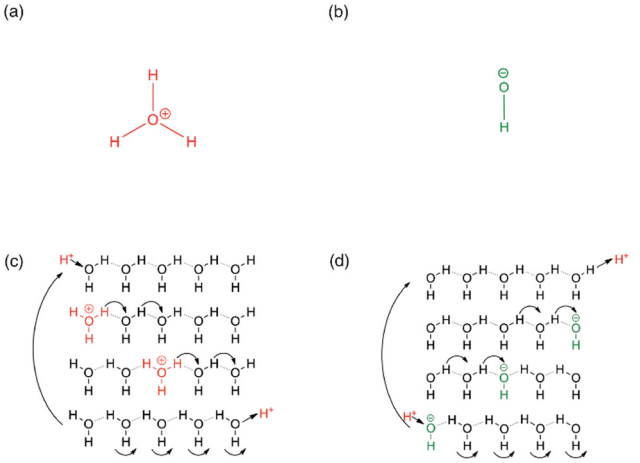

Fig. 3 (a) Hydronium ion (b) hydroxide ion (c) hop and turn Grotthus mechanism for the conductivity of H^+ as hydronium ion along a proton wire (d) Equivalent mechanism for OH^- conductivity as proton holes along a proton wire. Reproduced with permission from ref. 74.

Na^+.[73] This is a direct consequence of the specific interaction of protons with water molecules. In addition, considering its practical importance, the quantitative description of the proton transport mechanism has received significant interest, and it is conventionally described using two models: (i) the vehicle mechanism, or the direct diffusion of the proton carriers (*e.g.* H_3O^+ in water), is essentially a generic diffusion model valid to any solute, while (ii) the Grotthus mechanism takes into consideration the specific interactions that exist between protons and water molecules. In particular, according to the Grotthus mechanism, the protons are allowed to jump from one molecule capable of H-bonding (H_2O in this case) to a neighbouring one without the need for the significantly heavier O atom to move, resulting in an effective acceleration of the proton mobility. Thus, it is the favoured mechanism when fast ion transport is needed (Fig. 3).[74,75] In fact, Nafion®, the benchmark and commercial proton-exchange membrane integrated into PEM-FCs features proton conductivity pathways according to the Grotthus mechanism, in which, similar to the mechanism in aqueous solutions, protons are exchanged on clusters of H_2O and H_3O^+ that are supported by the membrane's sulphonic acid groups.[76] Such insights paved the way to developing MOFs with high proton conductivity. While initial studies were aimed at accelerating ion carriers; today, the focus has shifted to exploring channel spaces, capable of accommodating both the proton carriers and the conduction medium, *i.e.* H_3O^+ and H_2O. This approach effectively engineers proton conduction pathways from a crystallographic viewpoint.[50,77]

The mobility of hydroxide ions remains lower than that of protons, although the mobility of OH^- is significantly higher in aqueous solutions than that of other ionic solutes. It stands to reason that the exploitation of Grotthus- or Grotthus-like mechanisms should result in significantly improved hydroxide-ion conductivities in porous media, similarly to what has been observed for proton conductors (Fig. 3). In fact, theoretical calculations suggest the existence of a distinct transport mechanism, which may be viewed as an inverse proton transfer between the charge carrier OH^- and the H_2O conduction medium.[38]

Measuring hydroxide-ion transport

In the most general terms, mass transport in a particular medium is expressed through the self-diffusion coefficient. As such, mass transport in MOFs can be measured using a range of techniques; considering the large interaction cross-section of hydrogen with neutrons, neutron-based techniques in general, quasi-elastic neutron scattering (QENS) in particular is one of the most accurate and sensitive tools in determining the diffusion coefficient of hydroxide ions in a given material;[78] additionally, nuclear magnetic spin resonance (NMR) techniques are well suited in directly measuring dynamic effects in proton-bearing species such as OH^-, and pulsed-field gradient NMR spectroscopy is a powerful method in quantifying them.[79] Furthermore, other techniques, such as interference microscopy, infrared microscopy, luminescence quenching, quartz-crystal microbalance, and confocal laser scanning microscopy, have also been shown to yield diffusion coefficients in solids.[80–84]

Ion conductivity measurements at the same time are most typically carried out using electrochemical impedance spectroscopy, wherein a pellet, thin film, or membrane of the specimen is compressed to a known thickness and held in place between two electrodes under given conditions (temperature, electrolyte/relative humidity, and RH) under a set voltage within a particular frequency range under open circuit conditions. Effectively, the charge transference or the amount of charges passing through the specimen in the course of a certain duration is measured. Care must be taken for the piece of equipment to be in a controlled atmosphere, not only to ensure constant temperature and RH value throughout the experiment, both of which influence the OH^- conductivity, but also to avoid the $2\ OH^- + CO_2 \rightarrow CO_3^{2-} + H_2O$ reaction, as the technique normally relies on measuring 'any' ion transport. Thus, conductivity from CO_3^{2-} would also contribute to the measured value thereby burdening the experimental data with an additional yet unknown degree of error, in effect poisoning the fuel cell. Often, the Bode and Nyquist impedance plots are also acquired to apply the Nyquist semicircle method to calculate the charge transfer resistance and subsequently the conductivity.[85] It should be noted that experimental challenges arise from the MOF forms, as mentioned before, MOFs are typically synthesised as powders but for conductivity measurements, a free-standing form of them must be obtained. While significant progress has been made in MOF thin-film syntheses, this approach is not always available, practical or indeed convenient to determine bulk properties for instance on account of orientation effects;[61] at the same time, the precise measurement of the specimen width is crucial for accurate conductivity measurement, while the disintegration of the specimens also must be avoided, both of which are challenging with any of the MOF-forming methods.

MOF topologies in alkaline environments

As seen before, MOFs are promising materials for hydroxide ion-exchange membrane applications on account of their intrinsic electric insulating properties, inherent and tuneable ion-conductivity pathways, ability to be processed, *etc.*; however, major challenges include their stability in alkaline aqueous environments. In fact, electrolytes in AAEMFCs typically are made up of an aqueous KOH solution of 6–9 M in concentration, which evidently results in challenges to the stability of the exchange membrane regardless of the material classes used. In the case of metal–organic frameworks, there is limited information available as to which MOFs are stable in alkaline environments. Jiang *et al.* have assessed the current status and improvement strategies of the chemical stability of MOFs in a review paper, which may serve as a future inspiration and help identifying new directions in design tactics.[86] Although there is only very scarce data available on the stability of MOFs in the required pH range, some frameworks have been reported at pH $>$ 10, which may already be useful for evaluating the suitability of certain MOFs as hydroxide-ion exchange membranes for fuel cells.

It should be noted that the MOFs stable in alkaline conditions are very diverse both in terms of composition and topology, comprising O- and N-donor linkers, various transition metal nodes (both, single cations as well as oxidic clusters), as well as featuring 1D channels or 3D intersected channels. Most representatives of extremely high hydroxide-ion tolerance, *i.e.* stability at pH $\geq$ 14 are however high-pK_a azolate derivatives and relatively soft metals.[87] These most promising frameworks include PCN-601 (Ni_2TPP, H_4TPP – 5,10,15,20-tetra(1*H*-pyrazol-4-yl)porphyrin)[88] whose stability in saturated NaOH solution has been reported, ZIF-8 (ZnMeIM, MeIM – 2-methylimidazole) reportedly stable in 8 M NaOH solution at 100 °C,[89] as well as ZrPP-1 (PP = pyrogallic porphyrin), whose ability to withstand 20 M NaOH for a week[87] is outstanding and a highly promising prospect. In addition, PCN-602(Ni) (Ni_2TPPP, H_4TPPP - 5,10,15,20-tetrakis(4-(1*H*-pyrazol-4-yl)phenyl)porphyrin)[90] and La(BTB)H_2O (BTB = 1,3,5-tris(4-carboxyphenyl)benzene)[91] have also been shown to be stable at pH = 14, underlining their potential for exploitation in applications at highly basic conditions. Additionally, relatively common MOF topologies of MIL-101, MIL-53, and UiO-66[52] have demonstrated a degree of stability in alkaline media (pH = 12) and thus raising hopes for potential applications at high pH values.

As a more general design strategy, once again the HSAB (Hard and Soft Acid and Base Theory) principle[92] may be used as a guidance, high-valent metal cations combined with hard base oxidic donor ligands lead to strong coordination bonds extending framework stability, while low-valent metals combined with soft base N-heterocycles with high pK_a value favour the stability of the resultant coordination bonds, particularly in alkaline media. In addition, Jiang and co-workers have identified additional strategies to enhance the stability of MOFs in aqueous alkaline media, which include the use of several metals as a node, *i.e.* mixed-metal MOFs, introduction of azole-moieties in the carboxylic linkers, increasing hydrophobicity either *via* linker decoration with hydrophobic ligands or hydrophobic surface treatment, integration of (typically pyridinic) pillar ligands within the MOF structure, interpenetration, and compositing *e.g.* with carbonaceous materials or polymers.[86]

The above strategies fine-tune, in essence, weaken, the interactions between the framework and the medium, particularly those of hydroxide ions. Such approaches, alongside topological tuning of the framework, and, as seen, facilitating a Grotthus-like ion transport mechanism, are at the heart of controlling hydroxide-ion conductivity in a MOF and, perhaps not surprisingly, some of the very same strategies are being considered to maximise OH^- transport through MOF channels.

Considering that recent advances in (i) approaches for improving MOF stability in alkaline environments;[86] (ii) shaping and forming MOFs for more suitable mechanical characteristics[56–64] and new ways of improving static robustness;[93] (iii) more sustainable approaches to production;[67–70] and (iv) lowered costs[65,94] – all of which have been explored in excellent recent review papers. We identify the hydroxide-ion conductivity as the principal remaining bottleneck and therefore our continued discussion will be focussed on that.

Effecting OH^- transport in MOFs

Fundamentally, all strategies of tuning hydroxide-ion mobility in MOFs rely on the engineering of the interactions between the ions and the framework itself. Kitagawa *et al.* have put forward a three-level classification:[44]

Approach 1. To essentially introduce unbound and thus potentially mobile OH^- ions in the MOF channels is by the encapsulation of hydroxide-ion containing salts or ionic liquids (Fig. 4), as a result, both the cations and anions will be mobile and they both will migrate towards the oppositely charged electrodes when an external electric field is applied, this effectively reduces the overall number for hydroxide ions that transfer.

Approach 2. Hydroxide ion concentration may be intrinsically increased either by the direct synthesis or the post-synthetic modification[95] when the MOF itself is ionic, in this case positively charged scaffolds contain the OH^- counter-anions in their channels in their static form, *i.e.* when the frameworks experience no potential difference (Fig. 5). On the other hand, when there is an applied potential on the MOF, ion

Fig. 4 Schematic representation of the inclusion of an OH^- containing salt in a MOF's pores. Reproduced with permission from ref. 38.

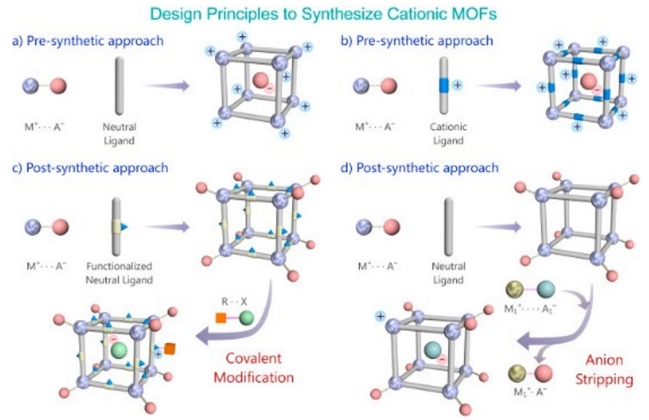

Fig. 5 Schematic representation of routes to build a cationic MOF *via* pre- and post-synthetic approach. Reproduced with permission from ref. 95.

transport is realised *via* the motion of the hydroxide ions down the potential gradient, along the MOF channels.

Approach 3. The third approach makes use of advances in the field of ion-conducting polymers, in which the polymers are inserted through the MOF channels[96] (Fig. 6), which effectively act as a host for the polymers displaying liquid-like free motion. This approach combines the flexibility and dynamic properties of the polymer guests with the directionality and robustness of the crystalline solid host MOF scaffolds.

In addition, the above approaches can also be combined with each other to increase both the hydroxide-ion concentration and mobility, and therefore effectively its transference number.

Analysis of OH^- conductivity data in MOFs

Table 1 summarises the hydroxide-ion conductivities in MOF-based materials measured to date at given conditions. Furthermore, it highlights which, if any, of the 3 approaches discussed above were used and whether additional specimen processing has been carried out. In addition to the main approaches to enhance ion conductivity, it should be recalled that for

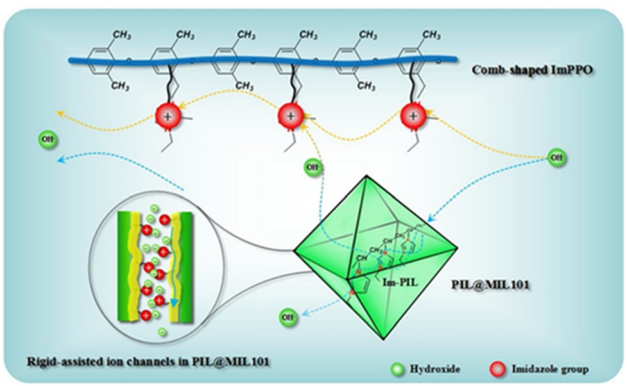

Fig. 6 Schematic illustration of the insertion of PILs into MOF channels and of hydroxide transport along the ion nanochannels. Reproduced with permission from ref. 96.

achieving high proton conductivity, the facilitations of the Grotthus mechanism had been successfully implemented, while there is some evidence that such a technique could also be employed for hydroxide-ion conductivity. It stands to reason to relate methodologies aimed at increasing MOF stability in alkaline media with those aimed at improving hydroxide ion conductivity on account of (i) the necessity for the MOF to be stable under the operating conditions and (ii) the fundamental analogy of engineering MOF-ion interactions.

First, it should be noted that the measurement conditions and sample production and processing methods are very different in most cases, and therefore, a straight-forward comparison of the results and subsequent drawing of conclusions are virtually impossible. Nevertheless, some considerations can be made, which can help identify further pathways to improving performance. In particular, the success of the various approaches and their combination applied to increasing hydroxide ion conductivity will be discussed below.

Topological and compositional remarks

From a compositional and topological perspective, one can notice a relative lack of diversity in the frameworks explored for hydroxide-ion conductivity so far. On account of the small number of MOF structures with demonstrated ability to withstand highly alkaline media, it should come as little surprise that most notable MOF topologies reported as hydroxide-ion conductive ones fall into the few more stable topologies and chemistries. Particularly, ZIF-8,[89] ZIF-67,[113] MIL-101,[114] and UiO-66[115] have been among the most studied frameworks. Interestingly, these frameworks that are not of these well-known and investigated families have compositional similarities, in the sense that they are all built up of (relatively) soft acids of Cu^+,[109] Ni^{2+}[110] or Ru^{2+}[112] combined with high pK_a heterocycles of 2,7-bis(3,5-dimethyl) dipyrazol-1,4,5,8-naphthalene-tetracarboxydiimide, 1,4-bis (pyrazol-4-yl)benzene-4-X (X = H, OH or NH_2), and 4,4′-dicarboxy-2,2′-bipyridine, respectively, which is in line with the HSAB theory.[92]

Approaches to induce OH^- conductivity and their combination

Among the hydroxide-ion conductors reported to date, the data on the conductivity of pure, *i.e.* non-modified or as-synthesised, MOFs are very scarce. However, some examples exist, including the conductivity of ZIF-8, NH_2-UiO-66(Zr), FJU-66 and a series of Ni-bis(pyrazol)benzene MOFs. Although these values are generally low, *e.g.* 2.3×10^{-9} S cm^{-1} in the case of the fairly hydrophobic ZIF-8,[38] other representatives have higher conductivities, including NH_2-UiO-66(Zr) with a remarkable performance of 2×10^{-3} S cm^{-1} in dark conditions,[107] when the formation of a hydrogen-bonded network of water molecules facilitated by the amino groups is unhindered. An interesting and somewhat contradictory effect was observed for the $[Ni_8(OH)_4(H_2O)_2(BDP\_X)_6]$ (H_2BDP_X = 1,4-bis(pyrazol-4-yl)benzene-4-X, X = H, OH, NH_2) metal–organic frameworks.[111] For these FCC MOFs, Navarro *et al.* observed a slight but measurable conductivity change as a function of the X ligand of the linker, intriguingly, the most hydrophobic ligand, *i.e.* H, displayed the highest conductivity and the worst performance was met by the most hydrophilic

Table 1 Hydroxide-ion conductivity in MOF-based materials at given relative humidity (RH) and temperature, including the MOF used, any additives such as salts or polymers inserted in the MOF pores, approach employed to enhance ion conductivity, membrane processing if applicable

MOF	Additive	Approach	Processing	σ (mS cm^{-1})	RH (%)	T (°C)	Ref.
ZIF-8 (Zn)	Cho-OH	1-IL	n/a	4×10^{-4}	98	25	97
		1-IL[a]	PVA membrane matrix	8.4×10^{-2}	98	60	
ZIF-8 (Zn)	Cho-OH	1-IL[a]	IL-templated synthesis + PVA membrane	2.6×10^{-1}	98	60	98
ZIF-8 (Zn)	BMIM-OH	1-IL	n/a	6.8×10^{-1}	98	80	99
	BMIM-OH	1-IL[a]	PVP/PVDF membrane blend	1	98	80	
ZIF-8 (Zn)	n/a	n/a	n/a	2.3×10^{-9}	>96	25	38
	Bu_4N-OH	1-IL		2.8×10^{-5}	>96		
	Bu_4N-OH + NaOH	1-IL + salt		6.2×10^{-4}	>96		
ZIF-8 (Zn)	Bu_4N-OH	1-IL[a]	PEI membrane	1	100	25	100
				1.46	100	55	
ZIF-8 (Zn) + ZIF-67 (Co) mixture	Bu_4N-OH	1-IL[a]	PEI membrane	1.5	100	25	
				2.7	100	55	
ZIF-67 (Co)	Bu_4N-OH	1-IL[a]	PEI membrane	1	100	25	
				1.5	100	55	
MIL-100 (Cr)–OH	n/a	2-Anion stripping from node	n/a	2.1×10^{-2}	99.9	50	101
NH_2-MIL-101 (Cr)	n/a	3	*N*-Vinylimidazole: *N*-vinyl-2-pyrrolidone/divinylbenzene Semi-interpenetrating membranes	120	—	80	102
MIL-101 (Cr)	Poly-*N*-vinylimidazolium	3[a]-PIL	SEBS binder used to prepare membrane of ImPEEK	36.6	—	20	103
MIL-101 (Cr)	Poly-1-vinyl-3-ethylimidzolium	3[a]-PIL	Comb-shaped ImPPO membrane	138	100	80	96
MIL-101 (Cr)	n/a	2[a]-linker modification	(Both polymer and MOF)	36	100	50	104
			ImPEEK membrane matrix	47	100	60	
NH_2-MIL-101 (Fe)-F	BPPO	2[a]-anion stripping	PVA coating covalently linked on the two sides	145	100	80	105
$[NH_2\text{-UiO-66 (Zr)}]^+Cl^-$	QA (PIL)	2 & 3[a]-Anion stripping then PIL	Membrane formation through casting with BPPO	123	100	80	106
NH_2-UiO-66 (Zr) w 10 eq. acetic acid of different ratios of an acetic acid modulator	n/a	n/a	Light OFF	$2 \times 10^{-\times 3}$	95	55	107
			Light ON	*ca.* 2×10^{-5}	95		
NH_2-UiO-66 (Zr)/Py-UiO-66(Zr)	n/a	2[a]-Linker modification	Im-PEEK	73	—	80	108
FJU-66 (Cu)	n/a	n/a	n/a	2.1×10^{-5}	95	30	109
	[EVIm]OH	1-IL		57	95	30	
				91	95	85	
	3 eq. KOH	1-Salt		6	95	30	
				59	95	85	
	0.9 eq. Bu_4N-OH	1-IL		1.99×10^{-4}	95	30	
				3.44×10^{-3}	95	85	
$[Ni_2(\mu\text{-pymca})_3]OH{\cdot}nH_2O$	n/a	2	n/a	8×10^{-1}	99	27	110
				2.5×10^{-2}	95	30	
				5.6×10^{-2}	95	90	
$[Ni_8(OH)_3(H_2O)(BDP\_H)_5]$	n/a	n/a	n/a	7.64×10^{-5}	22	40	111
$[Ni_8(OH)_3(H_2O)(BDP\_OH)_5]$	n/a	n/a	n/a	5.86×10^{-6}	22	40	
$[Ni_8(OH)_3(H_2O)(BDP\_NH_2)_5]$	n/a	n/a	n/a	7.32×10^{-5}	22	40	
$K[Ni_8(OH)_5(EtO)(BDP\_H)_{5.5}]$	KOH	1 & 2	PSM-missing linker	3.91×10^{-3}	22	40	

Table 1 (*continued*)

MOF	Additive	Approach	Processing	σ (mS cm^{-1})	RH (%)	T (°C)	Ref.
$K_3[Ni_8(OH)_3(EtO)(BDP\_O)_5$	KOH	1 & 2	PSM-missing linker	1.82×10^{-3}	0	40	
				2.75×10^{-2}	22	40	
				11.6	100	40	
$K[Ni_8(OH)_5(EtO)(BDP\_NH_2)_{5.5}]$	KOH	1 & 2	PSM-missing linker	3.73×10^{-5}	0	40	
				2.78×10^{-2}	22	40	
				1.47	100	40	
$Nd_7(OH)_5[Ru(dcbpy)_3]_4{\cdot}4nH_2O$	n/a	2	n/a	10^{-3}–10^{-4}	90	25	112
$Ce_7(OH)_5[Ru(dcbpy)_3]_4{\cdot}4nH_2O$	n/a	2			90	25	
$La_7(OH)_5[Ru(dcbpy)_3]_4{\cdot}4nH_2O$	n/a	2			90	25	
$Ln_7(OH)_5[Ru(dcbpy)_3]_4{\cdot}4nH_2O$	n/a	2		*ca.* 10^{-6}	40	25	

[a] Samples were further processed as membranes.IL-Ionic liquid; PIL-poly-ionic liquid; PSM-post-synthetic modification; Py-2,5-pyridinedicarboxylate; Pymca-pyrimidine-2-carboxylato; BDP_X-1,4-bis(pyrazol-4-yl)benzene-4-X (X = H, OH, NH_2); dcbpy-4,4′-dicarboxy-2,2′-bipyridine; Cho-choline; BMIM-1-butyl-3-methylimidazolium hydroxide; Bu_4N-tetrabutylammonium; BPPO-bromomethylated poly(2,6-dimethyl-1,4-phenylene oxide); QA-*N,N,N′,N′*-tetramethyl-1,6-hexanediamine and allyl bromide; EVIm-1-ethyl-3-vinylimidazolium; ImPPO-imidazolated poly (2,6-dimethyl-1,4-phenylene oxide); ImPEEK-imidazolated poly (ether ketone); PVA-polyvinyl alcohol; PVP-polyvinylpyrrolidone; PVDF-polyvinylidene fluoride; PEI-polyetherimide; SEBS-hydr. styrene-ethylene/butylene-styrene triblock copolymer

ligand, *i.e.* OH. While this observation was not explained in the manuscript, an attempt to interpret the results will be given later.

The rest of the conductivities reported so far have been measured on a specimen, which has been modified according to the approaches discussed previously. Generally speaking, MOFs built up of soft acids and heterocyclic linkers have been modified with Approach 1, some of which were combined with Approach 2, or with Approach 2 only. However, MOFs built up of hard acids and carboxylate linkers have either been modified with Approach 2 or Approach 3.

Approach 1. Two MOFs have been used to encapsulate ionic hydroxide-ion-containing species, ZIF-8[38,97–100] and FJU-66.[109] In the case of ZIF-8, ionic liquids have been reportedly added into the pores of the frameworks leading to significant OH^- conductivity enhancement; choline hydroxide (Cho-OH),[97,98] 1-butyl-3-methylimidazolium hydroxide (BMIM-OH),[99] and tetrabutylammonium hydroxide (Bu_4N-OH)[38,100] have all been explored with the highest ion conductivity recorded for BMIM-OH. However, it should be noted that the IL of the MOFs differed and not the same measurement conditions were applied, in particular, BMIM-OH@ZIF-8 was measured at 80 °C[99] whereas Cho-OH@ZIF-8[97,98] and Bu_4N-OH@ZIF-8[38,100] were measured at 25 °C, which may be the reason of the several orders of magnitude difference. At the same time, Cho-OH@ZIF-8 outperformed Bu_4N-OH@ZIF-8 by an order of magnitude under the same conditions. Choline ions are more hydrophilic than tetrabutylammonium ones, thus an increased extent of water adsorption may facilitate higher hydroxide-ion mobility, whereas $BMIM^+$ is highly hydrophobic. Apart from the question of hydrophobicity, it is also important to consider the strength of the interactions between the IL cation and the host framework. Considering that the OH^- counter-anion is principally interacting with the IL@MOF *via* electrostatic interactions, it stands to reason that their modulation would heavily impact ion mobility and thus the hydroxide-ion conductivity. Sadakiyo *et al.* suggested the formation of hydrophobic-hydrophobic interactions between the tetrabutylammonium ions and the methyl groups of the methyl-imidazolium linker in Bu_4N-OH@ZIF-8,[38] similar hydrophobic interactions and potentially some degree of π–π interactions between the methylimidazolium linker and the methylimidazolium moiety in $BMIM^+$ may also be the reason for its high hydroxide-ion mobility, *i.e.* loosely bonded anions. In addition, Sadakiyo and colleagues also measured the hydroxide ion conductivity of ZIF-8 treated with both Bu_4N-OH and NaOH,[38] the increased OH^- content led to a twenty-fold conductivity increase, highlighting the importance of encapsulation conditions and parameters.

The other framework topology explored for enhancing hydroxide-ion conductivity through the encapsulation of ionic species is the FJU-66. Here, Xiang and co-workers encapsulated two types of ILs, 1-ethyl-3-vinylimidazolium ($[EVIm]^+$) hydroxide and Bu_4N-OH, as well as KOH.[109] They found the addition of 1 eq. [EVIm]-OH yielded the highest ion conductivity of 91 mS cm^{-1} at 85 °C – a stunning, >5 orders of magnitude improvement over the empty framework, whereas the addition of 3 eq. of KOH resulted in somewhat lower but still high conductivity of 59 mS cm^{-1}. Interestingly, the addition of 0.9 eq. Bu_4N-OH resulted in comparatively low performance of 3.44×10^{-3} mS cm^{-1} under the same conditions. The authors attempted to rationalise these differences based on IL^+-MOF interactions being the strongest for $[EVIm]^+$ on account of its sp2 C and N atoms as possible binding sites to the naphthalene diimide groups on FJU-66 *via* hydrogen bonding or lone pair-π interactions, whereas K^+ are expected to be hydrated and thus offering a high concentration of localised H_2O molecules facilitating hydroxide-ion transport.[109]

Approach 2. To endow the frameworks with intrinsic positive charges and consequently with inherent OH^- content,

several strategies have been successfully applied, these include the direct synthesis of cationic frameworks, *e.g.* $Ln_7(OH)_5[Ru(dcbpy)_3]_4 \cdot 4nH_2O$[112] and $[Ni_2(\mu\text{-pymca})_3]OH \cdot nH_2O$,[110] where the charges are balanced by hydroxide ions in the MOF structures. In both of these cases, the positive charge is localised on the inorganic node. Additional charges around the nodes may be induced post-synthetically employing anion stripping, as was demonstrated by Feng *et al.* for MIL-100(Cr)[101] and successfully adapted for NH_2-MIL-101(Fe) by Xu and co-workers,[105] and for NH_2-UiO-66(Zr) by Tang and colleagues.[106] An alternative technique makes use of net positive charges created around the inorganic nodes through the absence of linkers that would otherwise balance the charges, *i.e.* the introduction of missing-linker defects, such as reported by Navarro *et al.* for their $[Ni_8(OH)_4(H_2O)_2(BDP\_X)_6]$ series.[111] On the other hand, the positive charges may also be generated on the linker, the two published examples both make use of post-synthetic modification. Jiang and colleagues achieved this through chloromethylation leading to the ultimate installation of imidazolium ions on the terephthalate linker of MIL-101(Cr),[104] while Wang and co-workers reported the oxidative methylation of nitrogen in 2,5-pyridinedicarboxylate using methyl iodine.[108] Among the above, the two cationic MOF representatives obtained by direct syntheses, *i.e.* $Ln_7(OH)_5[Ru(dcbpy)_3]_4 \cdot 4nH_2O$[112] and $[Ni_2(\mu\text{-pymca})_3]OH \cdot nH_2O$[110] have intrinsic hydroxide-ion content. $Ln_7(OH)_5[Ru(dcbpy)_3]_4 \cdot 4nH_2O$ frameworks (Ln = La, Ce, or Nd) in particular have rather low σ near ambient conditions though several orders of magnitude higher than what was observed for neutral frameworks, *cf.* 10^{-3}–10^{-4} mS cm^{-1} at 25 °C and 90%[112] RH compared with 2.3×10^{-9} mS cm^{-1} for the neutral ZIF-8 under similar conditions.[38] It is worth pointing out that hydroxide-ion conductivity in $Ln_7(OH)_5[Ru(dcbpy)_3]_4 \cdot 4nH_2O$ has a very significant dependence on the relative humidity, as a drop of 2–3 orders of magnitude has been observed when the RH% is from 90 to 40 at the same temperature.[112] This highlights the importance of water loading in the pores of MOFs and suggests that the preferred migration mechanism is more in line with the Grotthus mechanism than that of ion hopping. In the case of $[Ni_2(\mu\text{-pymca})_3]OH \cdot nH_2O$, similar but somewhat faster ion transport has been observed of *ca.* 10^{-2} mS cm^{-1} near ambient temperature and high RH%.[110] Interestingly, while a small increase in relative humidity resulted in a conductivity increase of a factor of 30 (8×10^{-1} mS cm^{-1} at 99% RH and 27 °C *vs.* 2.5×10^{-2} mS cm^{-1} at 95% RH and 30 °C), the temperature effect does not seem to be significant in this case (2.5×10^{-2} mS cm^{-1} at 30 °C and 56×10^{-2} mS cm^{-2} at 85 °C, both measurements carried out at RH = 95%), which once again suggests that H_2O molecules are actively participating in the hydroxide-ion carriage. Another pristine cationic MOF obtained by anion stripping is MIL-100(Cr)-OH, where the conductivity data measured at 50 °C and 99.9% RH is comparable with those mentioned above, suggesting a similar mechanism.[101] The remaining examples of cationic MOFs with OH^- counter-anions underwent additional processing and so their ion-conductivity performance will be discussed later.

Approach 3. There are only a few examples in which the insertion of ion-conducting polymers through the channels of MOFs has also been explored. In particular, poly-ionic liquids (PILs), *e.g.* *N*-vinylimidazole:*N*-vinyl-2-pyrrolidone with a small amount of divinylbenzene, poly *N*-vinylimidazolium,[102] and poly-1-vinyl-3-ethylimidazolium,[103,104] have been inserted into MIL-101(Cr) structures. In all cases, very high ion conductivities (> 30 mS cm^{-1}) were measured; however, the performances are difficult to compare on account of the very different measurement conditions and additives. It should be noted that for all examples at high temperatures, *i.e.* at 80 °C, the measured conductivity was outstanding, > 120 mS cm^{-1}, this is in line with what was previously observed for pure PILs,[116] suggesting that it is the PILs that appear to determine OH^- conductivity, while the MOF has more of a structural agency rather than an active role in the hydroxide-ion carriers.

Combination of different approaches. The above paragraphs provided a general overview of the three fundamentally different approaches to inducing hydroxide-ion conductivity in MOFs. In reality, however, these approaches may be combined or even overlapped. In fact, several examples may be found in which Approach 2 was combined with Approaches 1 and 3. The former case is adapted by Navarro and co-workers where $[Ni_8(OH)_4(H_2O)_2(BDP\_X)_6]$ (X = H, OH, or NH_2) MOFs have been post-synthetically modified to $K[Ni_8(OH)_5(EtO)(BDP\_X)_{5.5}]$ such as to create missing linker defects and thus creating net positive charges around the inorganic node, balanced by hydroxide ions (Fig. 7).[111] As the PSM is carried out using KOH as a base, some of it remains in the MOF channels thereby also potentially contributing to hydroxide-ion conductivity as an ionic guest material. When the effect of modification was compared with the pristine frameworks, *ca.* 3 orders of magnitude performance improvement was observed under the same conditions, regardless of the X-group (*ca.* 10^{-5} mS cm^{-1} *vs.* 3.9×10^{-3}–2.8×10^{-2} mS cm^{-1}). In addition, in the case of the X-ligands capable of H-bonding, *i.e.* OH and NH_2, the

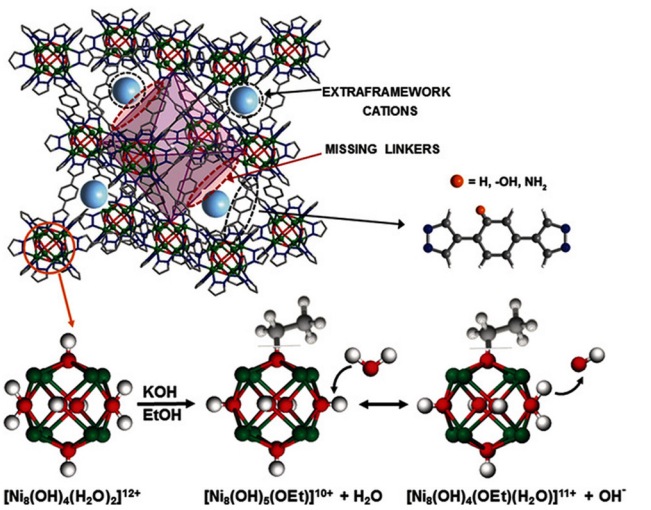

Fig. 7 Top: Schematic representation of the structure of the $K[Ni_8(OH)_5(EtO)(BDP\_X)_{5.5}]$ systems. Bottom: Cluster deprotonation taking place during the conversion into $K[Ni_8(OH)_5(EtO)(BDP\_X)_{5.5}]$ materials and proposed proton transfer mechanism to explain the ion conductivity of the hydrated materials. Figure reproduced with permission from [111].

hydroxide-ion conductivity of MOFs has also been explored as a function of relative humidity and a strong dependence has been found. In both cases, up to four orders of magnitude difference have been noted (X = OH 1.82×10^{-3} *vs.* 11.6 mS cm^{-1} at 0% and 100%, respectively, whereas for X = NH_2 3.73×10^{-5} *vs.* 1.47 mS cm^{-1}), once again highlighting the importance of the concentration of H_2O molecules as in the conductivity mechanism or as ion carriers. In fact, the values measured at 0% RH could provide a ballpark figure of the ion hopping contribution at the given temperature. Given the previous observation that the least hydrophilic ligand produced that best performance and the strong indication of a Grotthus mechanism is observed through RH%-dependent measurements, it is possible that additional, *e.g.* steric effects may also have a role in controlling OH^- conductivity in this MOF topology.

Approaches 2 and 3 have also been successfully combined by Tang *et al.* who prepared cationic NH_2-UiO-66(Zr)-OH *via* anion stripping, the channels of which were subsequently impregnated with the PIL precursors allyl bromide and *N,N,N′,N′*-tetramethyl-1,6-hexanediamine to form the PIL materials 'QA' *in situ*, inside the pores of MOFs.[106] The so-obtained QA@MOF was then further processed in the form of a membrane using brominated polyphenylene oxide. Similarly to other examples in which PILs have been introduced in the pores of MOFs, the measured OH^- conductivity was very high 123 mS cm^{-1} at 80 °C and 100% RH, similar to PIL performance, as seen before. Once again, it appears that the MOF plays the role more of a structural element than an active contributor to ion conductivity.

Further processing. While the effect of different approaches to inducing hydroxide-ion conductivity in MOFs has been reviewed above, the effect of further specimen processing needs to be evaluated as well. This is for two main reasons, (i) firstly, and this is perhaps self-explanatory, most MOFs are produced as polycrystalline powders, which are ill-suited to integration into any device, let alone as a self-supporting membrane – the formed ion-exchange membranes need to assume for their role in a fuel cell, and they must therefore be re-shaped and processed as a membrane; (ii) secondly, and this is perhaps a less evident consideration, according to Jiang *et al.* compositing of MOFs with other materials classes, including polymers, is one promising approach to improving stability in alkaline conditions,[86] as seen before, both purposes, *i.e.* improving MOF stability towards hydroxide ions as well as speeding up their transport in the MOF channels are fundamentally linked to MOF-OH^- interactions to a great extent. In this sense, for any effort to produce MOF-based membranes through compositing with another material, which is typically a polymer matrix, it is reasonable to assume that the ion conductivity would also be affected by the processing. As an example, in the case of IL@ZIF-8, some improvement of the hydroxide ion conductivity has been observed when the MOF particles were dispersed into polymer membranes: Cho-OH@ZIF-8 was composited with PVA to result in an increase of the conductivity from 4×10^{-4} mS cm^{-1} to 8.4×10^{-2} mS cm^{-1},[97] although caution must be exercised in the interpretation of these results as the MOF powders were measured at a lower temperature (25 °C *vs.* 60 °C in the case of the membrane). When the ZIF-8 crystals were formed using IL templated synthesis, filled with Cho-OH and dispersed in a PVA membrane, an additional improvement to 2.6×10^{-1} mS cm^{-1} has been observed at 60 °C.[97] Similarly, on using BMIM-OH as the IL, the PVP/PVDF polymer/MOF composite membrane outperformed the MOF powders in terms of hydroxide-ion conductivity as 6.8×10^{-1} mS cm^{-1} *vs.* 1 mS cm^{-1} at 80 °C and 98% RH.[99] In some cases, it is only the results obtained on the composites that have been recorded so the extent of improvement *vis-à-vis* the MOF powders cannot be evidenced.[100,103–106] Regardless, the experimental values are typically on the higher side, suggesting that some degree of improvement is likely. In addition, it is noteworthy that the ion conductivity for the Bu_4N-OH@ZIF-8/ZIF-67/ZIF-8 + ZIF-67 systems embedded in PEI membranes, generally good performances of 1–3 mS cm^{-1} have been observed at 100% RH, in particular, an 50–80% performance improvement has been observed for all three samples when the temperature was raised from 25–55 °C.[100] This is a relatively significant improvement, and it likely suggests that the ion hopping carrier mechanism is fairly prevalent in this system. MIL-101(Cr) has been infused with PILs and then integrated into the comb-shaped ImPPO membrane[104] or the ImPEEK membrane using a SEBS binder (Fig. 8).[103] In both of these cases, the very high hydroxide-ion conductivities were matching those observed in pure PIL materials.[116] The same observation can be made for membranes prepared from BPPO and anion-stripped PIL-infused NH_2-UiO-66(Zr)[106] by casting and from anion-stripped NH_2-MIL-101-Fe-F anchored on a BPPO film and sandwiched between PVA coatings on either side.[105] Once again, this suggests that MOFs act as a structural agent rather than the ion conductor. At the same time, Zhang *et al.* incorporated cationic NH_2-UiO-66(Zr) into an imidazole-functionalised PEEK matrix and demonstrated that the addition of cationic MOFs to the polymer matrix enhances its hydroxide ion conductivity at 80 °C, by almost a factor of 2 (44.3 mS cm^{-1} *vs.* 73 mS cm^{-1}),[108] although this value is somewhat lower than what was observed for the PIL@MOF composites,[102,103,105,106] it is a very high value regardless, one which highlights the synergy that can be

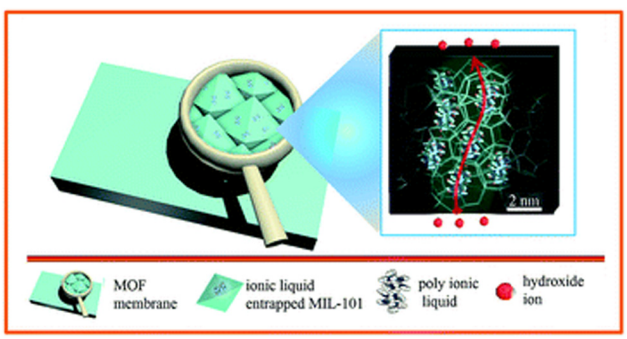

Fig. 8 Schematic illustration of *in situ* assembly of a poly(ionic liquid) in metal–organic framework. Reproduced with permission from ref. 103.

created by the adequate processing of cationic MOFs for hydroxide-ion exchange membrane applications. Nevertheless, it should be noted that the water content of these measurements was regulated in a very different approach, namely by immersing the membranes in deionised water for 24 h prior to measurements rather than controlling RH, therefore the resultant conductivity values are quite difficult to compare. In any case, these results give promise to ion-conductivity tuning *via* the processing of MOFs.

Conclusions and perspectives

To conclude, very high OH^- conductivities have been measured for MOF-based materials prepared in various approaches. To put the conductivity values into perspective, the proton conductivity of Nafion®, which exceeds 10 mS cm^{-1} up to 80 °C, can be used.[76] Considering that on account of its size, the transport of hydroxide ions compared with protons would be expected to be more sluggish. Therefore, one might consider $\sigma > 10$ mS cm^{-1} values determined under similar conditions (RH close to 100% and temperatures up to 80 °C) to be remarkable and promising ones. In fact, all three approaches for enabling hydroxide-ion conductivity, *i.e.* filling pores with hydroxide-ion conducting salts, formation of cationic frameworks with hydroxide counter-anions, and infiltration of hydroxide-ion conducting polymers into MOF pores, seen earlier have resulted in frameworks with high ion mobilities. Particularly spectacular results have been achieved for MOFs incorporating ion-conducting polymers in their channels; however, it appears that their conductivities are determined by the polymers themselves[116] and not the MOFs, whose role is likely more one of the structural agents. While this is of course highly interesting, it should be nevertheless considered whether MOFs are the best choice of materials for use as a mechanical agent alone. This role may be fulfilled by other materials, such as porous ceramics, which may be cheaper and more robust chemically and thermally. Currently, the other two approaches, both of which increase hydroxide-ion concentrations in the MOF pores, underperform the one relying on conducting polymers. However, there are some highly promising examples, wherein the ion conductivity of these MOFs approaches that of the polymers themselves. The most promising one involved the addition of IL [EVIm]OH into the pores of FJU-66, where $[EVIm]^+$ ions are strongly anchored in the MOF pores, presumably weakening the electrostatic interactions between the cations and the hydroxide ions, which renders them more mobility in the framework at high RH%.[109] The combination of engineering cationic MOFs through missing linker effects and concurrent KOH inclusion into MOFs also led to promising hydroxide-ion conductivities, specifically at high RH%. The significance of high RH% for OH^- conducting MOFs without PILs indicates that water molecules adsorbed on the MOF channels have a substantial importance. Such an effect suggests that the ion conductivity may be governed by the Grotthus mechanism, similarly to the proton conductivity. This is highly desirable because, as seen earlier, the Grotthus mechanism affords much lower activation energy (typically 2–3 kcal mol^{-1})[75] compared with the vehicular or *en masse* diffusion mechanism, in which the ions hop from one binding site to another.[117] What is surprising is that while for the development of proton-exchange membranes based on MOFs, significant effort has been put into nanochannel engineering for ensuring ion conductivity *via* the Grotthus mechanism,[51] such kind of rational MOF selection and/or engineering has not yet gained a foothold in the development of hydroxide-ion conducting MOFs. Perhaps the reason for this lies in the relatively poorer stability of most MOFs in alkaline conditions when compared with acidic media. On the other hand, there is some evidence that the structural processing of MOFs, *e.g.* as membranes, can also accelerate hydroxide-ion motions down a potential or concentration gradient. Interestingly, this is also one of the key suggestions for enhancing the MOF stability towards harsher alkaline conditions. Once again, this approach has not been knowingly explored, and consequently significantly verified and exploited to date. It is therefore hereby suggested that this could be an important future perspective in developing MOF-based hydroxide-ion exchange membranes. Additional strategies for improving the alkaline stability of MOFs include the use of mixed-metal MOFs, the introduction of azole moieties, and affecting framework interpenetration, all of which may have the potential in accelerating hydroxide ion conductivity as they modulate OH^--MOF interaction strengths. However, it should be noted that the ability to induce ion transport *via* the Grotthus mechanism appears to have by far the largest effect. It is for this reason that increasing hydrophobicity, one of the most promising methods to improve MOF stability towards alkaline conditions, will likely be counterproductive, as it would result in a lowered intrapore concentration of the ion-carrier water molecules.

It should be noted that the current status of hydroxide-ion conductivity in MOFs is relatively underdeveloped when compared with proton conductivity, for instance. This very well may be a direct consequence of PEMFC technology being more established than AAEMFCs, however, this relative lack of advance also comes with a less standardised way of data reporting and measurement conditions. As the ion conductivity performances depend strongly on variables such as temperature and relative humidity (or water concentration), reported results and thus performances would be more straightforward to compare if there were a standard set of conditions to carry out the experiments in.

Furthermore, in order to integrate MOF-based membranes into operational fuel cells, the crossover of gaseous molecules should be avoided. Although the polymer community regularly reports crossover data on ion-conducting polymer membranes,[118] such evaluations are completely absent for MOF ion conductors. It is hereby encouraged that techniques are adopted and/or developed to enable this important assessment of MOF materials for applications as ion-exchange membranes in fuel cells.

As a final thought, metal–organic frameworks still face a number of challenges to overcome before they can be

commercialised as integral parts of AAEMFCs. The three main challenges include the stability of MOFs in harsh alkaline media, their facile and scalable processing as membranes, as well as their affordability. Interestingly, one of the main conclusions of this critical review, namely the potential of the processing of MOFs *via* their compositing into polymer membranes could potentially simultaneously address all these challenges, therefore bringing the application of MOF-based OH^--exchange membranes closer to a commercial technology.

Author contributions

P. Á. Szilágyi conceptualised the remit of the manuscript, analysed the available literature data, wrote, reviewed, and edited the manuscript. M-M. Titirici contributed towards the conceptualisation through discussions.

Conflicts of interest

There are no conflicts to declare.

Acknowledgements

The authors would like to acknowledge funding from the Centre for Advanced Materials for Renewable Energy Generation (CAMREG #EP/P007805/1). PAS would like to acknowledge the financial support of the University of Oslo.

References

1 D. Bogdanov, M. Ram, A. Aghahosseini, A. Gulagi, A. S. Oyewo, M. Child, U. Caldera, K. Sadovskaia, J. Farfan, L. De Souza Noel Simas Barbosa, M. Fasihi, S. Khalili, T. Traber and C. Breyer, *Energy*, 2021, **227**, 120467.
2 H. Zsiborács, N. H. Baranyai, A. Vincze, L. Zentkó, Z. Birkner, K. Máté and G. Pintér, *Electronics*, 2019, **8**, 729.
3 C. E. Thomas, *Int. J. Hydrogen Energy*, 2009, **34**, 6005–6020.
4 A. Onorati, R. Payri, B. Vaglieco, A. Agarwal, C. Bae, G. Bruneaux, M. Canakci, M. Gavaises, M. Günthner, C. Hasse, S. Kokjohn, S.-C. Kong, Y. Moriyoshi, R. Novella, A. Pesyridis, R. Reitz, T. Ryan, R. Wagner and H. Zhao, *Int. J. Engine Res.*, 2022, **23**, 529–540.
5 L. Fan, Z. Tu and S. H. Chan, *Energy Reports*, 2021, **7**, 8421–8446.
6 Z. He, M. Cui, Q. Qian, J. Zhang, H. Liu and B. Han, *Proc. Natl. Acad. Sci. U. S. A.*, 2019, **116**, 12654–12659.
7 A. Züttel, A. Remhof, A. Borgschulte and O. Friedrichs, *Philos. Trans. R. Soc., A*, 2010, **368**, 3329–3342.
8 M. Yue, H. Lambert, E. Pahon, R. Roche, S. Jemei and D. Hissel, *Renewable Sustainable Energy Rev.*, 2021, **146**, 111180.
9 R. C. Thompson, C. J. Moore, F. S. vom Saal and S. H. Swan, *Philos. Trans. R. Soc., B*, 2009, **364**, 2153–2166.
10 J.-P. Lange, *ACS Sustainable Chem. Eng.*, 2021, **9**, 15722–15738.
11 M. Schoemaker, U. Misz, P. Beckhaus and A. Heinzel, *Fuel Cells*, 2014, **14**, 412–415.
12 S. Ahmad, T. Nawaz, A. Ali, M. F. Orhan, A. Samreen and A. M. Kannan, *Int. J. Hydrogen Energy*, 2022, **47**, 19086–19131.
13 M. K. Debe, *Nature*, 2012, **486**, 43–51.
14 L. Yang, J. Shui, L. Du, Y. Shao, J. Liu, L. Dai and Z. Hu, *Adv. Mater.*, 2019, **31**, 1804799.
15 D. R. Dekel, *J. Power Sources*, 2018, **375**, 158–169.
16 Z. F. Pan, L. An, T. S. Zhao and Z. K. Tang, *Prog. Energy Combust. Sci.*, 2018, **66**, 141–175.
17 V. Vijayakumar and S. Y. Nam, *J. Ind. Eng. Chem.*, 2019, **70**, 70–86.
18 A. Alaswad, A. Omran, J. R. Sodre, T. Wilberforce, G. Pignatelli, M. Dassisti, A. Baroutaji and A. G. Olabi, *Energies*, 2021, **14**, 144.
19 M. Shabani, H. Younesi, M. Pontié, A. Rahimpour, M. Rahimnejad and A. A. Zinatizadeh, *J. Cleaner Prod.*, 2020, **264**, 121446.
20 Y. Xing, H. Li and G. Avgouropoulos, *Materials*, 2021, **14**, 2591.
21 G. Kaur, V. Kumar, F. Baino, J. C. Mauro, G. Pickrell, I. Evans and O. Bretcanu, *Mater. Sci. Eng., C*, 2019, **104**, 109895.
22 R. K. Nagarale, G. S. Gohil, V. K. Shahi and R. Rangarajan, *Macromolecules*, 2004, **37**, 10023–10030.
23 C. Xu, R. Fang, R. Luque, L. Chen and Y. Li, *Coord. Chem. Rev.*, 2019, **388**, 268–292.
24 T. Jia, Y. Gu and F. Li, *J. Environ. Chem. Eng.*, 2022, **10**, 108300.
25 Ü. Anik, S. Timur and Z. Dursun, *Microchim. Acta*, 2019, **186**, 196.
26 J. F. Olorunyomi, S. T. Geh, R. A. Caruso and C. M. Doherty, *Mater. Horiz.*, 2021, **8**, 2387–2419.
27 L. G. Gordeeva, Y. D. Tu, Q. Pan, M. L. Palash, B. B. Saha, Y. I. Aristov and R. Z. Wang, *Nano Energy*, 2021, **84**, 105946.
28 M. J. Kalmutzki, C. S. Diercks and O. M. Yaghi, *Adv. Mater.*, 2018, **30**, 1704304.
29 P. Á. Szilágyi and A. J. Sobrido, *J. Energy Chem.*, 2022, **73**, 348–353.
30 S. Zhang, J. Wang, Y. Zhang, J. Ma, L. Huang, S. Yu, L. Chen, G. Song, M. Qiu and X. Wang, *Environ. Pollut.*, 2021, **291**, 118076.
31 A. S. Varela, W. Ju and P. Strasser, *Adv. Energy Mater.*, 2018, **8**, 1703614.
32 C. R. Groom, I. J. Bruno, M. P. Lightfoot and S. C. Ward, *Acta Crystallogr., Sect. B: Struct. Sci., Cryst. Eng. Mater.*, 2016, **72**, 171–179.
33 J. L. C. Rowsell and O. M. Yaghi, *Microporous Mesoporous Mater.*, 2004, **73**, 3–14.
34 Y. Ye, W. Guo, L. Wang, Z. Li, Z. Song, J. Chen, Z. Zhang, S. Xiang and B. Chen, *J. Am. Chem. Soc.*, 2017, **139**, 15604–15607.
35 A.-L. Li, Q. Gao, J. Xu and X.-H. Bu, *Coord. Chem. Rev.*, 2017, **344**, 54–82.
36 J. Li, M. Yi, L. Zhang, Z. You, X. Liu and B. Li, *Nano Sel*, 2022, **3**, 261–279.
37 M. Sadakiyo, T. Yamada, K. Honda, H. Matsui and H. Kitagawa, *J. Am. Chem. Soc.*, 2014, **136**, 7701–7707.
38 M. Sadakiyo, H. Kasai, K. Kato, M. Takata and M. Yamauchi, *J. Am. Chem. Soc.*, 2014, **136**, 1702–1705.

39 M. Sadakiyo and H. Kitagawa, *Dalton Trans.*, 2021, **50**, 5385–5397.
40 M. Sadakiyo, T. Yamada and H. Kitagawa, *J. Am. Chem. Soc.*, 2009, **131**, 9906–9907.
41 D. N. Dybtsev, V. G. Ponomareva, S. B. Aliev, A. P. Chupakhin, M. R. Gallyamov, N. K. Moroz, B. A. Kolesov, K. A. Kovalenko, E. S. Shutova and V. P. Fedin, *ACS Appl. Mater. Interfaces*, 2014, **6**, 5161–5167.
42 G. Alberti and M. Casciola, *Solid State Ionics*, 2001, **145**, 3–16.
43 X. Li, L. Dong, S. Li, G. Xu, J. Liu, F. Zhang, L. Lu and Y. Lan, *J. Am. Chem. Soc.*, 2012, **134**, 51–54.
44 J.-S. M. Lee, K.-i Otake and S. Kitagawa, *Coord. Chem. Rev.*, 2020, **421**, 213447.
45 D.-W. Lim and H. Kitagawa, *Chem. Rev.*, 2020, **120**, 8416–8467.
46 K. Biradha, A. Goswami, R. Moi and S. Saha, *Dalton Trans.*, 2021, **50**, 10655–10673.
47 X.-X. Xie, Y.-C. Yang, B.-H. Dou, Z.-F. Li and G. Li, *Coord. Chem. Rev.*, 2020, **403**, 213100.
48 Y. Ye, L. Gong, S. Xiang, Z. Zhang and B. Chen, *Adv. Mater.*, 2020, **32**, 1907090.
49 M. Sadakiyo, T. Yamada and H. Kitagawa, *ChemPlusChem*, 2016, **81**, 691–701.
50 D. I. Kolokolov, D.-W. Lim and H. Kitagawa, *Chem. Rec.*, 2020, **20**, 1297–1313.
51 D.-W. Lim, M. Sadakiyo and H. Kitagawa, *Chem. Sci.*, 2019, **10**, 16–33.
52 K. Leus, T. Bogaerts, J. De Decker, H. Depauw, K. Hendrickx, H. Vrielinck, V. Van Speybroeck and P. Van Der Voort, *Microporous Mesoporous Mater.*, 2016, **226**, 110–116.
53 D. Bůžek, S. Adamec, K. Lang and J. Demel, *Inorg. Chem. Front.*, 2021, **8**, 720–734.
54 J. Wei, D. Zhang, L. Zhang, H. Ouyang and Z. Fu, *ACS Appl. Mater. Interfaces*, 2019, **11**, 35597–35603.
55 J. O. Jensen, D. Aili, M. K. Hansen, Q. Li, N. J. Bjerrum and E. Christensen, *ECS Trans.*, 2014, **64**, 1175–1184.
56 Y. Dou, W. Zhang and A. Kaiser, *Adv. Sci.*, 2020, **7**, 1902590.
57 R. Ostermann, J. Cravillon, C. Weidmann, M. Wiebcke and B. M. Smarsly, *Chem. Commun.*, 2011, **47**, 442–444.
58 D. Zacher, O. Shekhah, C. Wöll and R. A. Fischer, *Chem. Soc. Rev.*, 2009, **38**, 1418–1429.
59 C. Crivello, S. Sevim, O. Graniel, C. Franco, S. Pané, J. Puigmartí-Luis and D. Muñoz-Rojas, *Mater. Horiz.*, 2021, **8**, 168–178.
60 S. Han and C. B. Mullins, *ChemSusChem*, 2020, **13**, 5433–5442.
61 Z.-G. Gu and J. Zhang, *Coord. Chem. Rev.*, 2019, **378**, 513–532.
62 J. Fonseca and T. Gong, *Coord. Chem. Rev.*, 2022, **462**, 214520.
63 D. G. Madden, D. O'Nolan, N. Rampal, R. Babu, C. Çamur, A. N. Al Shakhs, S.-Y. Zhang, G. A. Rance, J. Perez, N. P. Maria Casati, C. Cuadrado-Collados, D. O'Sullivan, N. P. Rice, T. Gennett, P. Parilla, S. Shulda, K. E. Hurst, V. Stavila, M. D. Allendorf, J. Silvestre-Albero, A. C. Forse, N. R. Champness, K. W. Chapman and D. Fairen-Jimenez, *J. Am. Chem. Soc.*, 2022, **144**, 13729–13739.
64 X.-M. Liu, L.-H. Xie and Y. Wu, *Inorg. Chem. Front.*, 2020, **7**, 2840–2866.
65 D. DeSantis, J. A. Mason, B. D. James, C. Houchins, J. R. Long and M. Veenstra, *Energy Fuels*, 2017, **31**, 2024–2032.
66 J. Ren, X. Dyosiba, N. M. Musyoka, H. W. Langmi, B. C. North, M. Mathe and M. S. Onyango, *Int. J. Hydrogen Energy*, 2016, **41**, 18141–18146.
67 G. Hoyez, J. Rousseau, C. Rousseau, S. Saitzek, J. King, P. Á. Szilágyi, C. Volkringer, T. Loiseau, F. Hapiot, E. Monflier and A. Ponchel, *CrystEngComm*, 2021, **23**, 2764–2772.
68 I. Pakamorė, J. Rousseau, C. Rousseau, E. Monflier and P. Á. Szilágyi, *Green Chem.*, 2018, **20**, 5292–5298.
69 M. C. Ribadeneyra, J. King, M. M. Titirici and P. Á. Szilágyi, *Chem. Commun.*, 2022, **58**, 1330–1333.
70 M. Titirici, S. G. Baird, T. D. Sparks, S. M. Yang, A. Brandt-Talbot, O. Hosseinaei, D. P. Harper, R. M. Parker, S. Vignolini, L. A. Berglund, Y. Li, H.-L. Gao, L.-B. Mao, S.-H. Yu, N. Díez, G. A. Ferrero, M. Sevilla, P. Á. Szilágyi, C. J. Stubbs, J. C. Worch, Y. Huang, C. K. Luscombe, K.-Y. Lee, H. Luo, M. J. Platts, D. Tiwari, D. Kovalevskiy, D. J. Fermin, H. Au, H. Alptekin, M. Crespo-Ribadeneyra, V. P. Ting, T.-P. Fellinger, J. Barrio, O. Westhead, C. Roy, I. E. L. Stephens, S. A. Nicolae, S. C. Sarma, R. P. Oates, C.-G. Wang, Z. Li, X. J. Loh, R. J. Myers, N. Heeren, A. Grégoire, C. Périssé, X. Zhao, Y. Vodovotz, B. Earley, G. Finnveden, A. Björklund, G. D. J. Harper, A. Walton and P. A. Anderson, *J. Phys.: Mater.*, 2022, **5**, 032001.
71 E. G. Schlosser, *Chem. Ing. Tech.*, 1978, **50**, 244.
72 S. Qiu, M. Xue and G. Zhu, *Chem. Soc. Rev.*, 2014, **43**, 6116–6140.
73 P. Atkins, P. W. Atkins and J. de Paula, *Atkins' physical chemistry*, Oxford university press, 2014.
74 T. Miyake and M. Rolandi, *J. Phys.: Condens. Matter*, 2015, **28**, 023001.
75 N. Agmon, *Chem. Phys. Lett.*, 1995, **244**, 456–462.
76 H. G. Haubold, T. Vad, H. Jungbluth and P. Hiller, *Electrochim. Acta*, 2001, **46**, 1559–1563.
77 D.-W. Lim and H. Kitagawa, *Chem. Soc. Rev.*, 2021, **50**, 6349–6368.
78 N. Rosenbach Jr., H. Jobic, A. Ghoufi, F. Salles, G. Maurin, S. Bourrelly, P. L. Llewellyn, T. Devic, C. Serre and G. Férey, *Angew. Chem., Int. Ed.*, 2008, **47**, 6611–6615.
79 F. Stallmach, S. Gröger, V. Künzel, J. Kärger, O. M. Yaghi, M. Hesse and U. Müller, *Angew. Chem., Int. Ed.*, 2006, **45**, 2123–2126.
80 J. Kärger, T. Binder, C. Chmelik, F. Hibbe, H. Krautscheid, R. Krishna and J. Weitkamp, *Nat. Mater.*, 2014, **13**, 333–343.
81 C. Wang and W. Lin, *J. Am. Chem. Soc.*, 2011, **133**, 4232–4235.
82 O. Zybaylo, O. Shekhah, H. Wang, M. Tafipolsky, R. Schmid, D. Johannsmann and C. Wöll, *Phys. Chem. Chem. Phys.*, 2010, **12**, 8093–8098.
83 W. Zhou, C. Wöll and L. Heinke, *Materials*, 2015, **8**, 3767–3775.

84 S. Han, T. M. Hermans, P. E. Fuller, Y. Wei and B. A. Grzybowski, *Angew. Chem., Int. Ed.*, 2012, **51**, 2662–2666.
85 P. Vadhva, J. Hu, M. J. Johnson, R. Stocker, M. Braglia, D. J. L. Brett and A. J. E. Rettie, *ChemElectroChem*, 2021, **8**, 1930–1947.
86 M. Ding, X. Cai and H.-L. Jiang, *Chem. Sci.*, 2019, **10**, 10209–10230.
87 E.-X. Chen, M. Qiu, Y.-F. Zhang, Y.-S. Zhu, L.-Y. Liu, Y.-Y. Sun, X. Bu, J. Zhang and Q. Lin, *Adv. Mater.*, 2018, **30**, 1704388.
88 K. Wang, X.-L. Lv, D. Feng, J. Li, S. Chen, J. Sun, L. Song, Y. Xie, J.-R. Li and H.-C. Zhou, *J. Am. Chem. Soc.*, 2016, **138**, 914–919.
89 K. S. Park, Z. Ni, A. P. Côté, J. Y. Choi, R. Huang, F. J. Uribe-Romo, H. K. Chae, M. O'Keeffe and O. M. Yaghi, *Proc. Natl. Acad. Sci. U. S. A.*, 2006, **103**, 10186–10191.
90 X.-L. Lv, K. Wang, B. Wang, J. Su, X. Zou, Y. Xie, J.-R. Li and H.-C. Zhou, *J. Am. Chem. Soc.*, 2017, **139**, 211–217.
91 J. Duan, M. Higuchi, S. Horike, M. L. Foo, K. P. Rao, Y. Inubushi, T. Fukushima and S. Kitagawa, *Adv. Funct. Mater.*, 2013, **23**, 3525–3530.
92 R. G. Pearson, *J. Chem. Educ.*, 1968, **45**, 581.
93 P. Z. Moghadam, S. M. J. Rogge, A. Li, C.-M. Chow, J. Wieme, N. Moharrami, M. Aragones-Anglada, G. Conduit, D. A. Gomez-Gualdron, V. Van Speybroeck and D. Fairen-Jimenez, *Matter*, 2019, **1**, 219–234.
94 X. Dyosiba, J. Ren, N. M. Musyoka, H. W. Langmi, M. Mathe and M. S. Onyango, *Sustainable Mater. Technol.*, 2016, **10**, 10–13.
95 A. Karmakar, A. V. Desai and S. K. Ghosh, *Coord. Chem. Rev.*, 2016, **307**, 313–341.
96 J. Chen, M. Guan, K. Li and S. Tang, *J. Ind. Eng. Chem.*, 2021, **94**, 465–471.
97 C. Liu, S. Feng, Z. Zhuang, D. Qi, G. Li, C. Zhao, X. Li and H. Na, *Chem. Commun.*, 2015, **51**, 12629–12632.
98 C. Liu, G. Zhang, C. Zhao, X. Li, M. Li and H. Na, *Chem. Commun.*, 2014, **50**, 14121–14124.
99 T. Zhang, G. Yu, X. Liang, N. Zhao, F. Zhang and F. Qu, *Int. J. Hydrogen Energy*, 2019, **44**, 14481–14492.
100 J. Vega, A. Andrio, A. A. Lemus, L. F. del Castillo and V. Compañ, *Electrochim. Acta*, 2017, **258**, 153–166.
101 C. Mao, R. A. Kudla, F. Zuo, X. Zhao, L. J. Mueller, X. Bu and P. Feng, *J. Am. Chem. Soc.*, 2014, **136**, 7579–7582.
102 N. Anahidzade, M. Dinari, A. Abdolmaleki, K. F. Tadavani and M. Zhiani, *Energy Fuels*, 2019, **33**, 5749–5760.
103 Z. Li, W. Wang, Y. Chen, C. Xiong, G. He, Y. Cao, H. Wu, M. D. Guiver and Z. Jiang, *J. Mater. Chem. A*, 2016, **4**, 2340–2348.
104 X. He, M. Gang, Z. Li, G. He, Y. Yin, L. Cao, B. Zhang, H. Wu and Z. Jiang, *Sci. Bull.*, 2017, **62**, 266–276.
105 B. Wu, L. Ge, D. Yu, L. Hou, Q. Li, Z. Yang and T. Xu, *J. Mater. Chem. A*, 2016, **4**, 14545–14549.
106 K. Li, J. Chen, M. Guan and S. Tang, *Int. J. Hydrogen Energy*, 2020, **45**, 17813–17823.
107 S. Wang, S. Fan, Z. Fang, Y. Hu, M. Dong and X. Peng, *ACS Appl. Nano Mater.*, 2021, **4**, 8352–8359.
108 J. Ren, J. Xu, M. Ju, X. Chen, P. Zhao, L. Meng, J. Lei and Z. Wang, *Advanced Powder Materials*, 2022, **1**, 100017.
109 Z. Li, Z. Zhang, Y. Ye, K. Cai, F. Du, H. Zeng, J. Tao, Q. Lin, Y. Zheng and S. Xiang, *J. Mater. Chem. A*, 2017, **5**, 7816–7824.
110 S. S. Nagarkar, B. Anothumakkool, A. V. Desai, M. M. Shirolkar, S. Kurungot and S. K. Ghosh, *Chem. Commun.*, 2016, **52**, 8459–8462.
111 C. Montoro, P. Ocón, F. Zamora and J. A. R. Navarro, *Chem. – Eur. J.*, 2016, **22**, 1646–1651.
112 A. Watanabe, A. Kobayashi, E. Saitoh, Y. Nagao, S. Omagari, T. Nakanishi, Y. Hasegawa, W. M. Sameera, M. Yoshida and M. Kato, *Inorg. Chem.*, 2017, **56**, 3005–3013.
113 R. Banerjee, A. Phan, B. Wang, C. Knobler, H. Furukawa, M. O'Keeffe and O. M. Yaghi, *Science*, 2008, **319**, 939–943.
114 G. Férey, C. Mellot-Draznieks, C. Serre, F. Millange, J. Dutour, S. Surblé and I. Margiolaki, *Science*, 2005, **309**, 2040–2042.
115 J. H. Cavka, S. Jakobsen, U. Olsbye, N. Guillou, C. Lamberti, S. Bordiga and K. P. Lillerud, *J. Am. Chem. Soc.*, 2008, **130**, 13850–13851.
116 E. Abouzari-Lotf, M. V. Jacob, H. Ghassemi, M. Zakeri, M. M. Nasef, Y. Abdolahi, A. Abbasi and A. Ahmad, *Sci. Rep.*, 2021, **11**, 3764.
117 P. Ramaswamy, N. E. Wong and G. K. H. Shimizu, *Chem. Soc. Rev.*, 2014, **43**, 5913–5932.
118 Q. Tang, B. Li, D. Yang, P. Ming, C. Zhang and Y. Wang, *Int. J. Hydrogen Energy*, 2021, **46**, 22040–22061.